Supporting Information

A Simple Decagram-Scale Synthesis of an Atomically Dispersed, Hierarchically Porous Fe–N–C Catalyst for Acidic ORR

Burak Koyuturk[a,=], Eliyahu M. Farber[b,=], Friedrich E. Wagner[c], Tim-Patrick Fellinger[a,d]*, David Eisenberg[b]*

Synthesis

Magnesium iminodiacetate (Mg-IDA) was prepared according to previous reports on MOCPs.[1,2] 15.97 g of iminiodiacetic acid (IDA, 0.12 mol) were added to 300 mL DI, preheated to 85 °C in a 2 L beaker and stirred until the IDA dissolved entirely. Then 11.66 g of basic magnesium carbonate (0.096 mol) were added, and a white solid material precipitated. The solution was stirred for 15 minutes, transferred to an ice bath, and 1.5 L of ethanol were added. The precipitate was allowed to settle overnight, then the liquid was decanted, and the sample was dried at 50 °C for 3 days. Mg-IDA samples were obtained with a yield of 50% (assuming 1:1 Mg:IDA ratio). Mg-IDA, a white powder, was put into a quartz boat and loaded into a tube furnace. The material was heated to 70 °C for 1 hour under a flow of argon, and then to temperature T (800, 850, 900, 950 °C) for 1 hour, then allowed to cool down to room temperature. The carbon was washed in 150 mL of 1 M HCl overnight (to remove the MgO), then filtered, neutralized with copious amounts of DI water and dried overnight at 50 °C. Transmetalation with Fe was carried out by refluxing the washed carbon in a 50 mM $FeCl_2$ methanol (200 ml solution per 100 mg catalyst) solution at 80 °C, followed by an acidic work-up with 0.1 M HCl and deionized water. Transmetalated samples were dried in the oven at 80 °C. The scaled-up synthesis of [Fe(N/C)_900] was performed by quintupling the synthesis of Mg-IDA, and then repeating it. About 200 g of Mg-IDA were obtained, and subsequently heated (in 4 batches) to 900 °C under argon using the same profile as described above. The obtained fine black powder was washed in 1 M HCl, rinsed with deionized water, and dried. The Fe coordination was carried out with the following change: 2 L of 50 mM anhydrous $FeCl_2$ in methanol were used per 5 gr catalyst. During the transmetalation methanol was lost via evaporation and the final volume of carbon suspension in methanol was approximately 1 L.

Materials characterization

Thermal gravimetric analysis (TGA) was performed in a Netzsch Jupiter STA 449F3 instrument, under argon flow (20 mL min^{-1}), at a heating rate of 1 °C min^{-1}. TGA-MS experiments were performed with TGA/DSC 1 and THERMO Star Gas analysis system (Pfeiffer Vacuum) instruments, equipped with a gas controller (GC 200, Mettler Toledo Corp., Switzerland). Mg-IDA-800 sample was heated up to 950 °C following the same heating conditions as the synthesis (heating ramp, inert gas, drying temperature etc.). Powder X-ray diffraction (XRD) was recorded on a Rigaku SmartLab instrument operating at 45 kV and 150 mA, at a wavelength of 1.54 Å. N_2 gas sorption was measured on a Quantachrome Autosorb iQ porosimeter. The samples were outgassed approximately 12 hours at 150 °C prior to the measurements. The isotherms were acquired between p/p_0 of 10^{-5} and $p=p_0$. BET surface areas were calculated using the ASiQwin software. The pore size distribution, micropore volume and micropore

surface area were determined by slit/cylindrical/sphere pore model of Quenched Solid Density Functional Theory (QSDFT) method. Total pore volume was calculated from the uptake at p/p_0 ~ 0.99. Raman spectroscopy was performed on a Horiba LabRam HR Evolution Raman microscope using 10× lens, 532 nm laser excitation wavelength, and 1800 grating. The length of the graphitic domain was calculated

using $$L_a(nm) = (2.4 \cdot 10^{-10}) \cdot \lambda^4 \cdot \left(\frac{I_D}{I_G}\right)^{-1}$$.[3] X-Ray photoelectron spectroscopy (XPS) samples were prepared by depositing a sample on copper tape, and the spectra was collected on a PHI VersaProbe III scanning microprobe supplied from Physical Instruments at UHV ~ 10^{-10} torr with step size of 0.05 eV. The charge correction was applied using the C 1s position (284.7 eV). Deconvolution was performed in CasaXPS software. High resolution scanning electron microscopy was done on a Zeiss ultra+ at 3 kV and an in-lens detector. High resolution scanning electron microscopy was done on a Titan Themis G2 60-300 at 80 kV and a high angle annular dark field (HAADF) detector. Mössbauer spectra were recorded with a sinusoidal velocity waveform at room temperature and at 4.2 K with 112mg/cm^2 of the catalyst enclosed in a lucite holder. For the low-temperature measurement, both the absorber and the ^{57}Co in rhodium source were cooled in a liquid helium bath cryostat. The fitting of the spectrum was carried out with MOS90 software (version 2.2). The isomer shifts given in Table S2 are relative to α-Fe at room temperature. The total iron content of the sample was estimated from the total intensity, i.e., the total area under the 4.2 K Mössbauer pattern by comparison with a spectrum of a hematite absorber of known thickness measured under the same conditions and assuming that the recoil-free fractions of all components in the Mössbauer spectrum of the catalyst are the same as that of hematite. The accuracy of the method is limited and may have an error of ~20%.

Electrochemical Measurements

The catalyst dispersion (ink) was prepared by dispersing the catalyst powder in dimethylformamide (DMF) and adding the ionomer (Nafion © 5 wt% in mixture of aliphatic alcohols and water) followed by 20 min sonication. In a typical ink preparation, 2 mg sample and 47.2 µL ionomer were dispersed in 652 µL DMF and after 20 min sonication, 13.7 µL ink was dropcasted on glassy carbon (working electrode) aiming at 200 µg/cm2 catalyst loading. A rotating gold disk electrode was used as working electrode (WE) for the stability measurements.
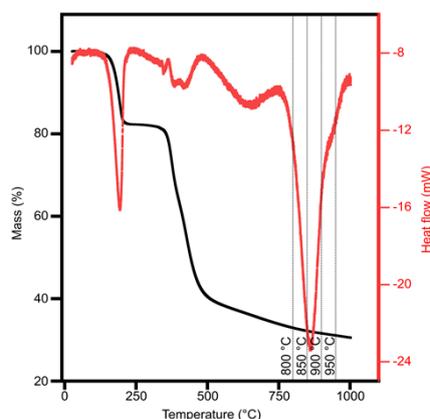
Figure S1. TGA-DSC of magnesium iminodiacetate. Pyrolysis temperatures chosen for the synthesis are indicated by vertical dotted lines.
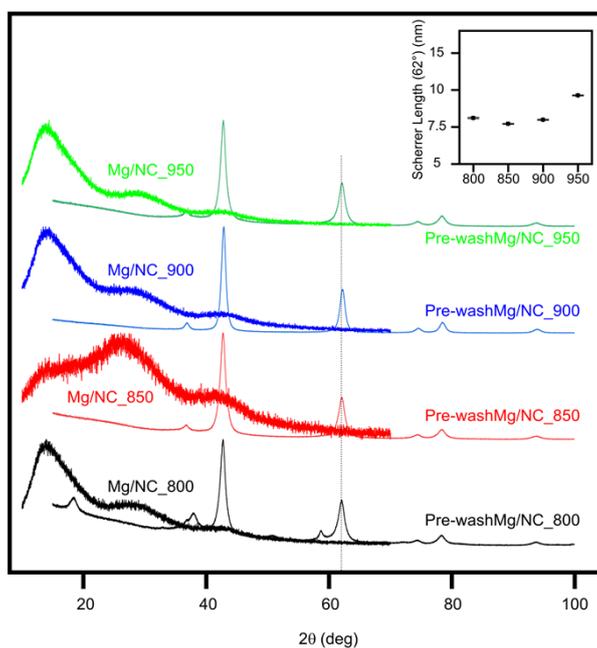

Figure S2. pXRD measurements for the pre-wash Mg/NC samples, compared with the samples after the wash. Scherrer analysis results for pre-wash Mg/NC samples is in the inset, measured for the diffraction peak at 62°; three other diffraction peaks showed identical trends.
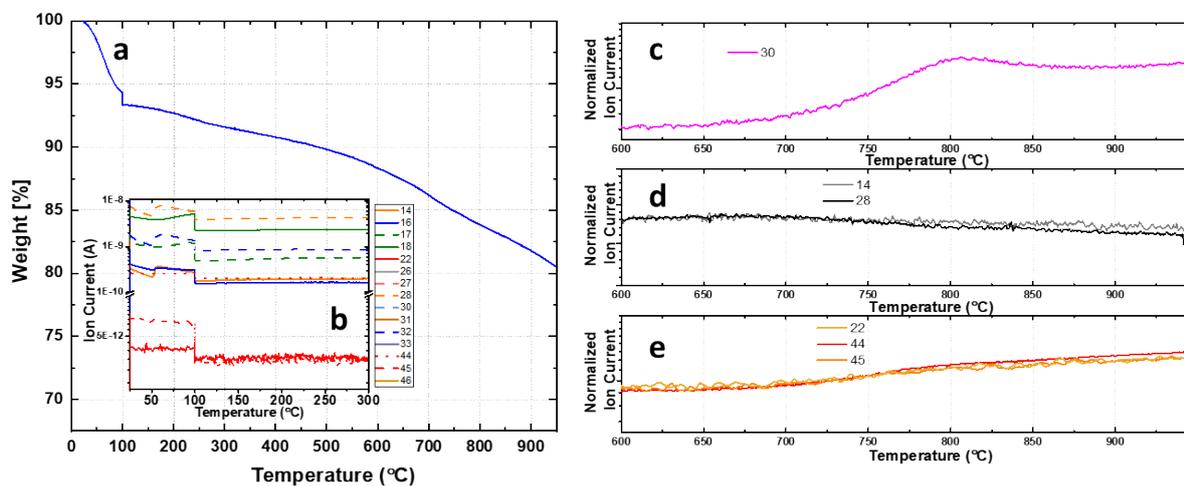

Figure S3. TGA-MS traces of heat-treated Mg/NC_800; (a) TGA, (b) MS traces between 25–300 °C, (c,d,e) Normalized MS signals for m/z of 30-14, 28-22, 44, 45.

Table S1. Elemental analysis results for Mg/NC samples (before Fe transmetalation) measured by ICP-MS.

Sample	wt% C	wt% N	wt% O	wt% Mg
Mg/NC_800	83.72	6.36	7.41	0.20
Mg/NC_850	82.02	10.40	5.97	0.18
Mg/NC_900	84.10	8.90	5.49	0.13
Mg/NC_950	85.86	7.11	5.33	0.22

Table S2. Mössbauer fitting parameters for each component of [Fe(NC_900)] for the spectrum measured at 4.2 K.

.Assignment	Quadrupole Splitting (QS, mm/s)	Isomer Shift (IS, mm/s)	Hyperfine Field (HF, Tesla)	Relative Area (RA, %)
D1	1.18	0.46		0.43
D3	3.73	0.95		0.12
Sextet		0.48	47.6	0.45

Table S3. D1 relative content in the Fe–N–C literature.

| D1 %	T (K)	Reference
43	**4.2**	**This work, [Fe(NC_900)]**
89	5	Chemical vapour deposition of Fe–N–C oxygen reduction catalysts with full utilization of dense Fe–N$_4$ sites[4]
62	5	Evolution Pathway from Iron Compounds to Fe(II)–N$_4$ Sites through Gas-Phase Iron during Pyrolysis[5]
44.4	4.2	Resolving the Dilemma of Fe–N–C Catalysts by the Selective Synthesis of Tetrapyrrolic Active Sites via an Imprinting Strategy[6]
37.1	4.2	Active-Site Imprinting: Preparation of Fe–N–C Catalysts from Zinc Ion–Templated Ionothermal Nitrogen-Doped Carbons[7]
68.1	298	Effect of Ball-Milling on the Oxygen Reduction Reaction Activity of Iron and Nitrogen Co-doped Carbide-Derived Carbon Catalysts in Acid Media[8]
58	298	Identification of catalytic sites for oxygen reduction in iron- and nitrogen-doped graphene materials[9]
58	298	Fe–N–C electrocatalyst with dense active sites and efficient mass transport for high-performance proton exchange membrane fuel cells[10]
58	298	Unravelling the Nature of Sites Active toward Hydrogen Peroxide Reduction in Fe–N–C Catalysts[11]
53	298	Degradation by Hydrogen Peroxide of Metal-Nitrogen-Carbon Catalysts for Oxygen Reduction[12]
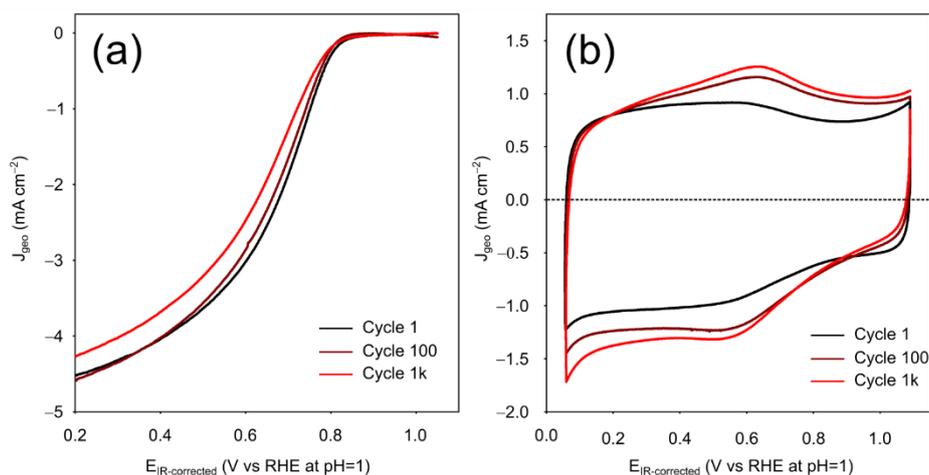
Figure S4. Carbon corrosion test results for [Fe(NC_900)]: (a) LSV at 1600 rpm, (b) CV. Recorded in O_2-saturated and N_2-saturated 0.1 M HClO4 (respectively) after 1, 100, and 1000 cycles.

Table S4. Activity indicators and material properties of small and large scale syntheses of Fe(N/C_900)] and Mg(NC_900).

Sample	E_{onset} (V)	$E_{1/2}$ (V)	I_D/I_G (Mg(N/C_900)	SSA	V_{total} (cm^3/g)	N wt% (ICP-MS)	Fe wt% (Mössbauer)
Small scale (0.1 gr)	0.83	0.69	1.43	1614	1.62	7.82	0.79
Large scale (10.1 gr)	0.85	0.70	1.44	1323	1.75	7.64	-

Single cell PEM-FC tests:

Although the scope of the present report is the scalable synthesis of a promising Fe-N-C catalyst, the possibility to utilize the catalysts in PEM fuel cell measurements is herein shown. [Fe(N/C_900)] was heated up to 950 °C with a heating ramp of 10 K/min and held for 30 min. The resulting sample was denoted as [Fe(N/C_900_950)]. The MEAs were prepared by catalyst coated membrane (CCM) employing decal transfer technique and coating PTFE (polytetrafluoroethylene) foil with the catalyst, aiming for at a loading of 2 mg/cm^2. The polarization curve obtained in O_2-H_2 under differential flow configuration shows promising activity, with an unexpectedly high OCP (0.93 V) and a current density of 7 mA/cm^2 at 0.9 V. The activity at low current density region points out the fast kinetics of [Fe(N/C_900_950)] whereas electrode design parameters and resistances dominate at high current densities.

The iR-corrected polarization curve is shown in Figure S5. The kinetic region of the polarization curve shows comparable activities for [Fe(N/C_900_950)] to commercial PGM-free catalyst. The mass activities extracted from the iR-corrected cell voltages at 0.8 V and

0.9 V are 32.1 A/g and 3.6 A/g for [Fe(N/C_900_950)], respectively, indicating good kinetics parameters despite the relatively low Fe content in [Fe(N/C_900_950)].
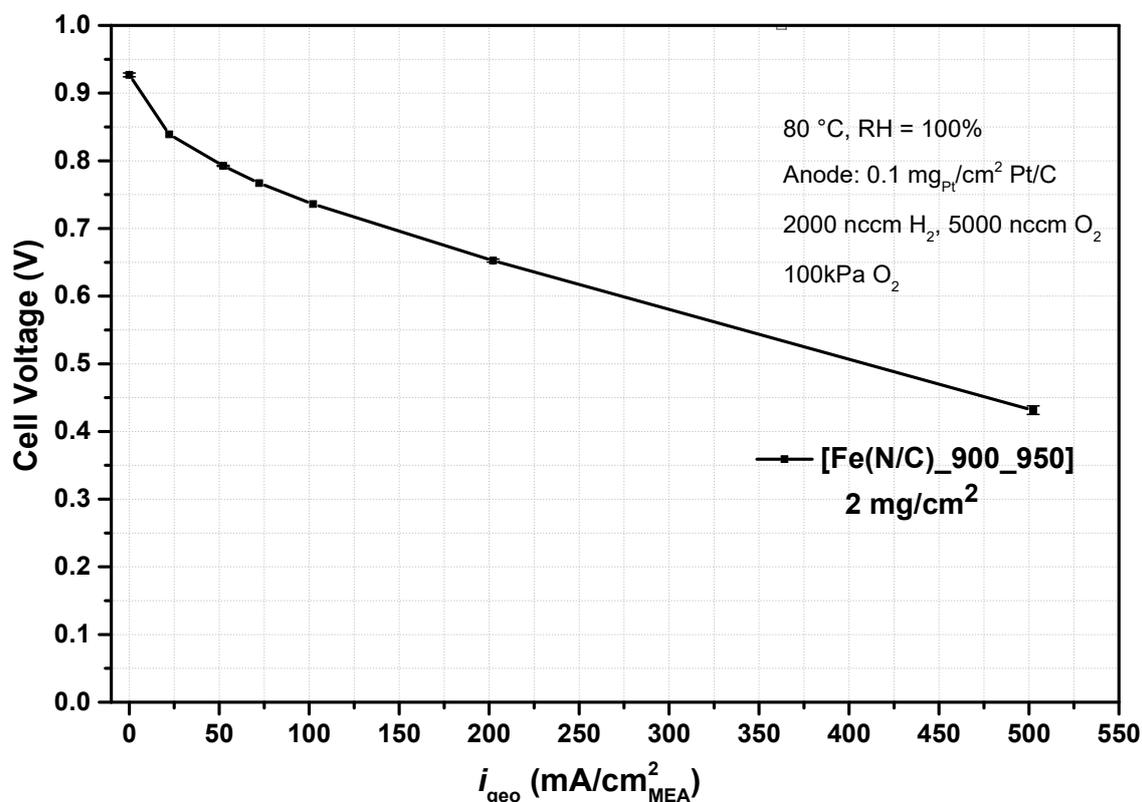

Figure S5. Single-cell test results for [Fe(N/C_900_950)] under differential flow conditions: 2000 nccm H_2 in anode, 5000 ncccm O_2 in cathode with P_{O_2}=100 kPa and a relative humidity of 100% at T=80 °C. The catalyst loadings used for anode and cathode are 0.1 mg_{Pt}/cm^2 and 2 mg/cm^2 respectively. The polarization curve was recorded after a holding time of 5 min before determining points at each current density.

References

1 D. Eisenberg, W. Stroek, N. J. Geels, C. S. Sandu, A. Heller, N. Yan and G. Rothenberg, *Chem.–Eur. J.*, 2016, **22**, 501–505.

2 E. M. Farber, K. Ojha, T. Y. Burshtein, L. Hasson and D. Eisenberg, *Mater. Adv.*, 2020, **1**, 20–33.

3 M. B. Vázquez-Santos, E. Geissler, K. László, J.-N. Rouzaud, A. Martínez-Alonso and J. M. D. Tascón, *J. Phys. Chem. C*, 2012, **116**, 257–268.

4 L. Jiao, J. Li, L. L. Richard, Q. Sun, T. Stracensky, E. Liu, M. T. Sougrati, Z. Zhao, F. Yang, S. Zhong, H. Xu, S. Mukerjee, Y. Huang, D. A. Cullen, J. H. Park, M. Ferrandon, D. J. Myers, F. Jaouen and Q. Jia, *Nat. Mater.*, 2021, **20**, 1385–1391.

5 J. Li, L. Jiao, E. Wegener, L. L. Richard, E. Liu, A. Zitolo, M. T. Sougrati, S. Mukerjee, Z. Zhao, Y. Huang, F. Yang, S. Zhong, H. Xu, A. J. Kropf, F. Jaouen, D. J. Myers and Q. Jia, *J. Am. Chem. Soc.*, 2020, **142**, 1417–1423.

6 D. Menga, J. L. Low, Y.-S. Li, I. Arčon, B. Koyutürk, F. Wagner, F. Ruiz-Zepeda, M. Gaberšček, B. Paulus and T.-P. Fellinger, *J. Am. Chem. Soc.*, 2021, **143**, 18010–18019.

7 D. Menga, F. Ruiz-Zepeda, L. Moriau, M. Šala, F. Wagner, B. Koyutürk, M. Bele, U. Petek, N. Hodnik, M. Gaberšček and T.-P. Fellinger, *Advanced Energy Materials*, 2019, **9**, 1902412.

8 S. Ratso, M. T. Sougrati, M. Käärik, M. Merisalu, M. Rähn, V. Kisand, A. Kikas, P. Paiste, J. Leis, V. Sammelselg, F. Jaouen and K. Tammeveski, *ACS Appl. Energy Mater.*, 2019, **2**, 7952–7962.

9 A. Zitolo, V. Goellner, V. Armel, M.-T. Sougrati, T. Mineva, L. Stievano, E. Fonda and F. Jaouen, *Nature Mater*, 2015, **14**, 937–942.

10 X. Wan, X. Liu, Y. Li, R. Yu, L. Zheng, W. Yan, H. Wang, M. Xu and J. Shui, *Nat Catal*, 2019, **2**, 259–268.

11 C. H. Choi, W. S. Choi, O. Kasian, A. K. Mechler, M. T. Sougrati, S. Brüller, K. Strickland, Q. Jia, S. Mukerjee, K. J. J. Mayrhofer and F. Jaouen, *Angewandte Chemie International Edition*, 2017, **56**, 8809–8812.

12 V. Goellner, V. Armel, A. Zitolo, E. Fonda and F. Jaouen, *Journal of The Electrochemical Society*, 2015, **162**, H403–H404.